Molecular Crystals and Liquid Crystals
Publication details, including instructions for authors and subscription information:
http://www.tandfonline.com/loi/gmcl20

Alignment Properties of Liquid Crystal on Etched Anodic Aluminum Oxide Film

Tsung-Ta Tang [a], Che-Hsuan Li [a] & Ru-Pin Pan [a]
[a] Department of Electrophysics, National Chiao Tung University, Hsinchu, Taiwan, R.O.C.
Published online: 14 Jun 2011.

To cite this article: Tsung-Ta Tang, Che-Hsuan Li & Ru-Pin Pan (2011) Alignment Properties of Liquid Crystal on Etched Anodic Aluminum Oxide Film, Molecular Crystals and Liquid Crystals, 544:1, 100/[1088]-111/[1099], DOI: 10.1080/15421406.2011.569282

To link to this article: http://dx.doi.org/10.1080/15421406.2011.569282

Mol. Cryst. Liq. Cryst., Vol. 544: pp. 100/[1088]–111/[1099], 2011

ISSN: 1542-1406 print/1563-5287 online
DOI: 10.1080/15421406.2011.569282

Alignment Properties of Liquid Crystal on Etched Anodic Aluminum Oxide Film

TSUNG-TA TANG, CHE-HSUAN LI, AND RU-PIN PAN

Department of Electrophysics, National Chiao Tung University, Hsinchu, Taiwan, R.O.C.

Anodic aluminum oxide (AAO) is a widely studied material with self-assembled nanochannel which is perpendicular to the substrate with nanometer-scale diameters and high aspect ratios. It is used for protecting the aluminum surface or as dielectric material. In this work, the alignment properties of liquid crystal on the etched AAO thin films were studied. By controlling the etching time, not only the pore sizes but also the thickness of the etched AAO thin films can be modified. Both homeotropic and homogenous alignment properties have been demonstrated on the etched AAO thin films with controlling etching time.

Keywords Anodic aluminum oxide; liquid crystals; vertical alignment

1. Introduction

The liquid crystal panels have been widely used in the modern display applications, such as liquid crystal displays, liquid crystal projectors, and liquid crystal televisions. One of the most important elements of liquid crystal panels is the alignment layers. It provides the boundary condition to align the liquid crystal molecules uniformly at the surface along a particular designed orientation without any external field. Depending on different alignment layers, the liquid crystal molecules orient homogenously or homeotropically. The homogenous alignment can be obtained by rubbing polyimide films [1], ion-beam bombardment method [2,3], photo-alignment method [4,5] and using the microgrooved substrates [6–9]. The homeotropic alignment can be obtained by coating the substrate with hydrophobic films such as Silone compounds or the ferromagnetic film. The SiO_x oblique evaporation method can give any of the homogenous, homeotropic and tilted alignments by controlling the evaporation angle [10–12]. On the other hand, the liquid crystal molecules can be aligned based on molecular interaction or surface morphology.

Anodic aluminum oxide (AAO) is a widely studied material that is used for protecting aluminum surface or as dielectric material in microelectronics application. AAO has been studied extensively over five decades [13]. There are two kinds of

Address correspondence to Ru-Pin Pan, Department of Electrophysics, National Chiao Tung University, Hsinchu 30010, Taiwan, R.O.C. Tel.: +886-3-5731989; Fax: +886-3-5725230; E-mail: rpchao@mail.nctu.edu.tw

AAO, the nonporous barrier oxide and the porous oxide. When aluminum layer is anodized in neutral or basic solutions, a flat, nonporous, featureless insulating barrier oxide is fabricated. When aluminum is anodized in an acid electrolyte (pH < 5), the pore arrays can be fabricated with diameters varying between 5 and 100 nm. The diameter of pores depends on the pH value of the electrolyte, the anodizing voltage and the different electrolyte, such as sulfuric, phosphoric, chromic, citric, oxalic acid, etc. [14–16]. The porous AAO film has been reported to be a typical self-assembled nanochannel material [17,18]. It exhibits a homogenous morphology with hexagonal columnar structures which grow perpendicular to the substrate with nanometer-scale diameters and interpore spacings. Such films present uniform pore sizes (between 10 nm and several 100 nm), high pore densities (ranging from 10^9 to $10^{12}\,cm^{-2}$), and high aspect ratios (>20). By using the porous AAO as templates, various nanometer sized materials, including metals, semiconductors, organics and polymers, have been reported [19–21].

There are several significant properties of AAO materials. It is an inorganic and porous material, and almost transparent and colorless in visible region. According to these properties, AAO film is a good candidate as the alignment layer of liquid crystal displays. T. Maeda and K. Hiroshima had demonstrated the vertical alignment of liquid crystal molecules on AAO films [22,23]. In our previous work [24], the pore sizes of the AAO films can be controlled by using different anodizing voltages. The conoscopic pattern, the pretilt angle and the polar anchoring strength of the liquid crystal cells with non-uniform and uniform porous AAO thin film have been examined. It is shown that all these different AAO films are good vertical alignment layers. However, the anchoring strength depends on anodizing condition. Recently, we also sucessfully integrated the porous AAO thin film and liquid crystal on the ITO glass substrate for applying the external electric field [25]. The demonstrated liquid crystal panel has a transmittance of 60–80%, and the threshold voltage is $3\,V_{rms}$ with a response time of 62.5 ms.

In this work, the alignment characterizations of the etched AAO thin films with different etching time have been studied. By using the etched AAO film as the alignment layer, both homeotropic and homogenous alignment of the liquid crystal cell have been demonstrated. In order to investigate the alignment mechanism, the morphology and the transmittance of the etched AAO thin film have been measured in Section 3.1 and 3.2. After using the etched AAO thin films as the alignment layers, the transmitted and conoscopic images of the liquid crystal cell, and the polar anchoring strength have been observed in Section 3.3 and 3.4. Finally, a possible alignment mechanism has been proposed in Section 3.5.

2. Experimental Methods

2.1. *Sample Preparation*

Figure 1 shows the scheme of the preparation procedure of the etched AAO thin film with different etching time. The porous AAO is formed by anodizing aluminum thin film or aluminum foil in acid electrolytes. The display-grade glass substrates (Wintek Corporation, Taiwan) coated with indium tin oxide (ITO) on one side were used. The AAO films were fabricated on the side of the substrates without the ITO coating. First, a pure aluminum (99.99%) films were evaporated on the cleaned glass substrates by a thermal coating system. The thickness of the aluminum film was about

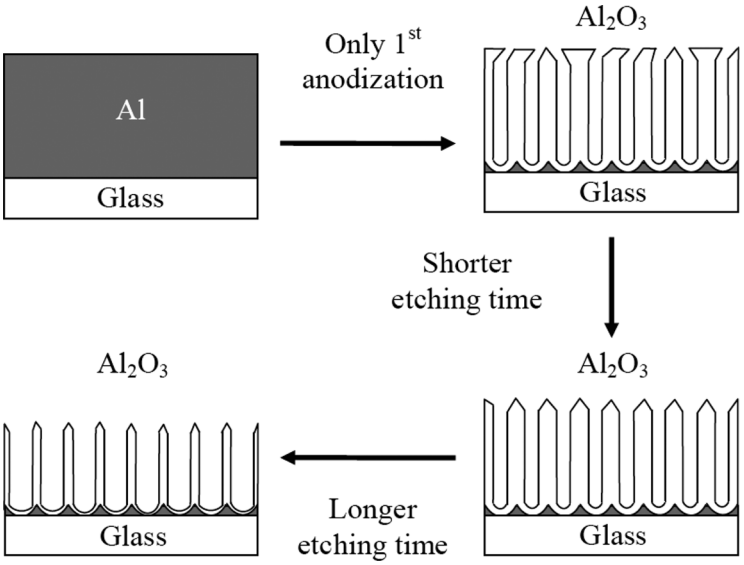

Figure 1. the scheme of the preparation procedure of the etched AAO thin film.

500 nm. Then, the aluminum film was anodized under a constant voltage with 3 wt% oxalic acid ($H_2C_2O_4$) aqueous solution in a home-made electrochemical trough. The temperature of the anodic solution was controlled at 6.0 ± 0.5°C. A platinum plate was used as the cathode. By using a voltage sourcemeter (Model 2410 sourcemeter, Keithley), the dc anodizing voltage was controlled at 40 V and the anodizing current was monitored simultaneously.

After the anodizing process finished, the AAO thin film was etched by a mixture of chromic acid (1.5 wt% H_2CrO_4) and phosphoric acid (6 wt% H_3PO_4) at 60°C. The etching time was controlled between 1.5 minutes and 6.0 minutes. The etching process not only etchs the AAO thin film from top to bottom, but also thins out the wall of the AAO cylinder. By this process, the thickness and the pore diameter of AAO thin film both can be modified.

2.2. *Examining Methods*

By using the field emission scanning electron microscope (FESEM: HITACHI S-4700i), the morphology and the nanostructure of the porous AAO thin film were observed. All of the AAO thin films were evaporated thin platinum layer to reduce charging effects. The thickness of AAO thin film can be measured by examining the cross-view of the AAO FESEM image.

In order to use the AAO thin film as the alignment layer, the transmittance of AAO thin films in visible region are very important. The transmittance of AAO thin films are taken by using a UV-Visible spectrometer (Oceanoptics, model ISS-UV-VIS and USB2000) with air as the reference.

Finally, the alignment characterization of the AAO thin film is necessary to be investigated. The investigative liquid crystal cell is made by putting together a pair of glass substrates with the AAO film face to face. The nematic liquid crystal, 5CB (from Merck co.), was filled into the cell in the isotropic phase (above 36°C). The

thickness of liquid crystal layers is 23 μm. The liquid crystal alignment in the cell is examined with a polarizing microscope. The cell is put between a pair of crossed polarizers. By using the polarizing microscope, the transmitted image and the conoscopic image can be examined at the nematic phase (room temperature, around 25°C). The conoscopy is a useful optical method to analyze the alignment of the uniaxial crystals by observing the interference image [26]. Furthermore, the polar anchoring strength characterizes the surface energy ability out of the substrate plane. By applying the magnetic field on the vertical alignment cell, the polar anchoring strength can be determined from the transmittance, which is a function of applied magnetic field above the threshold magnetic field [27].

3. Results and Discussion

3.1. *Morphology of the Etched Anodic Aluminum Oxide Surface*

Figure 2 shows the FESEM image of the etched AAO thin film with different etching time. The top view images are shown in left column, and the side view images are shown in right column. When the etching time is 0 minute, the FESEM image (Fig. 2, part 1) also shows the fine crack-like structures connecting irregular small pores. After immersing the AAO thin film in the etching solution, the nanoporous structure is appeared in FESEM image. When the etching time increased, the pore diameter significantly increased and the thickness of the wall of the AAO cylinder decreased. In addition, at 3.0 minutes, the FESEM image (Fig. 2, part 2) shows a different image. There are some clusters of nanorods with some hexagonal curve on the bottom of these clusters. When the etching time is longer than 3.0 minutes, the wall of the cylinder is too thin to maintain the cylindrical structure. According to Figure 2, part 3, it shows that the cylindrical structure collapsed and the hexagonal curve surface still remained when the etching times are longer than 3.5 minutes. Although the cylindrical structure was broken down, the porous structure still remains and the walls of cylinder become thousands of nanotip structures.

Figure 3 shows the relationship between the diameters of the pores and the etching time. Batch A and Batch B are fabricated with the same condition. The pore sizes of AAO thin films of Batch A and Batch B are consistent. If the etching time is less than 3.0 minutes, the pore sizes are almost proportional to etching time. When the AAO thin films were etched with longer etching time, the pore sizes become larger. However, the etching time is longer than 3.0 minutes, the pore diameters slightly decrease from 92 nm to 81 nm.

According to the side view image, it is easy to measure the thickness of the etched AAO thin film with different etching time, shown in Figure 4. The thickness of the AAO thin film etched with between 1.5 and 3.0 minutes remain around 450 nm. The thickness has a sudden drop at 3.5 minutes. When the etching time is longer than 3.5 minutes, the thickness becomes less than 50 nm.

3.2. *Transmittance of the Anodic Aluminum Oxide Layer*

In order to use the AAO thin film as an alignment layer, the transmittance of the AAO thin film in the visible region is significantly important. Figure 5 shows the transmittance of the AAO films on the ITO glass substrate as a function of wavelength from 300 to 1000 nm. The cut off wavelength at 350 nm is due to absorption

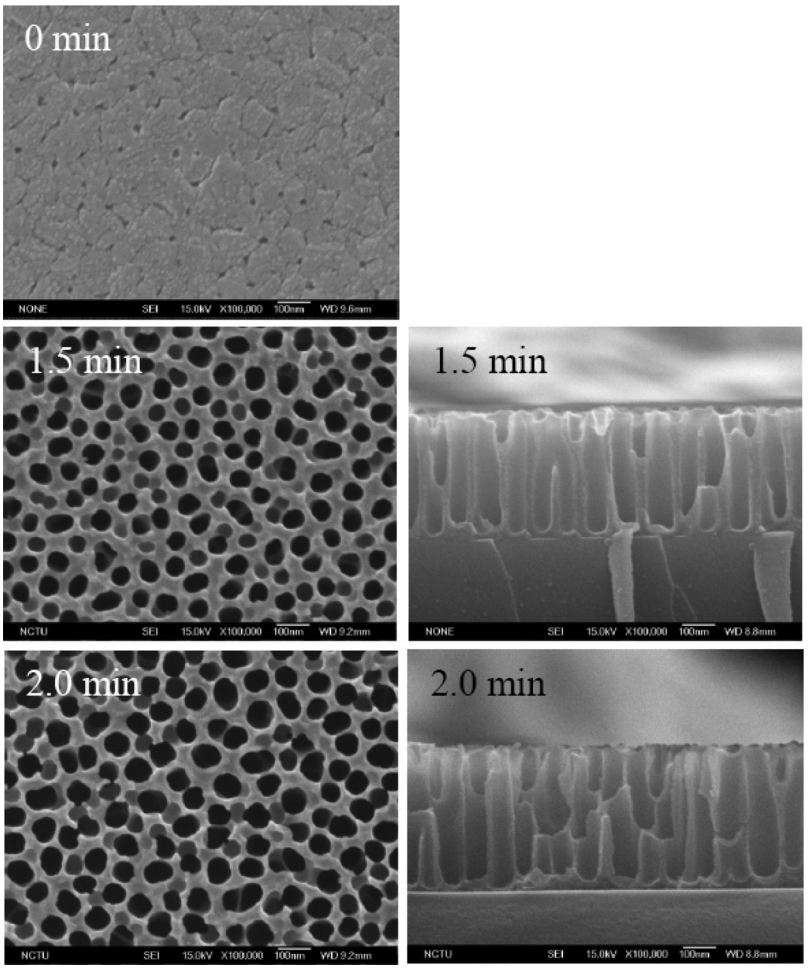

Figure 2 (Part 1). The FESEM image of the etched AAO thin film with different etching time, 0 min, 1.5 min, and 2.0 min.

of the ITO glass substrate. For all etched AAO films with different etching time, the transmittance is about 65% over this spectral range. In comparison, the transmittance of the substrates with ITO thin film on the back side is around 80%. In Figure 5(a), the ripples of the spectral transmittance for the AAO films with the etching time between 0.0 and 3.0 minute are attributed to the interference effects of the films which thickness are around 450 nm. When the etching time is longer than 3.5 minutes, the AAO surfaces only remain the nanotips structure and there is no ripple in the spectrum. According to the transmittance, all of the etched AAO thin films are highly transparent in the visible region.

3.3. *Alignment Characterization*

According to the previous work [24], the un-etched AAO thin film can provide the vertical alignment for the nematic liquid crystal. Figures 6(a) and (b) show the polarizing transmitted images of the liquid crystal cells with the different etched

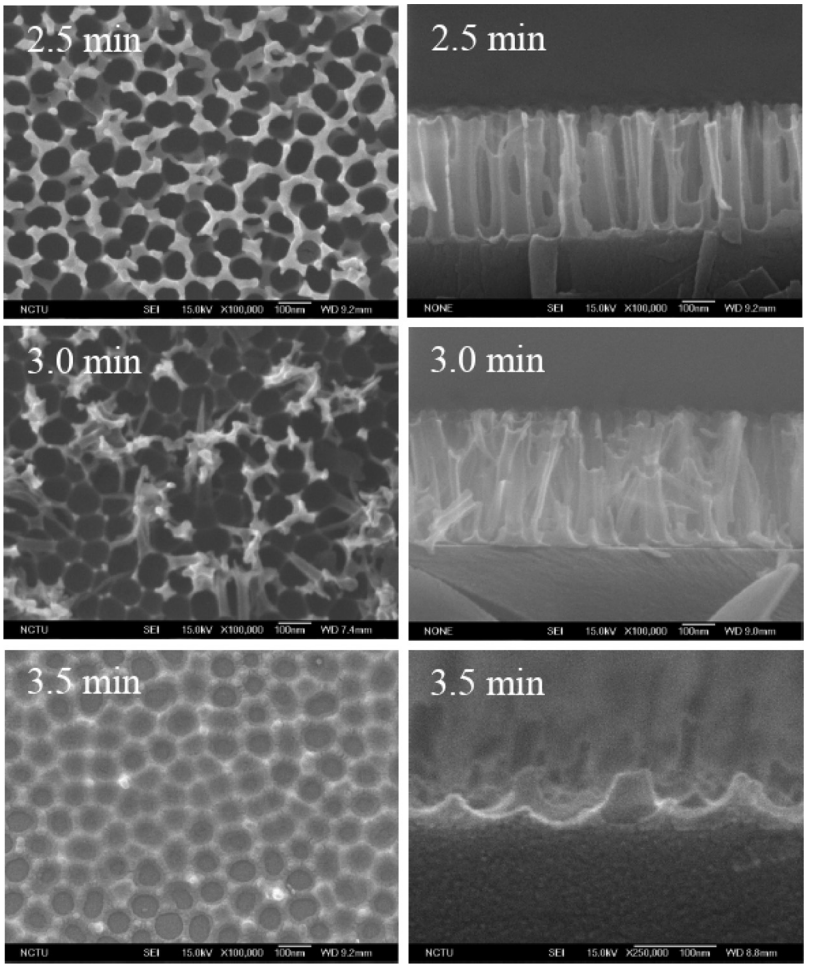

Figure 2 (Part 2). Continued, with etching time, 2.5 min, 3.0 min, and 3.5 min.

AAO thin films as alignment layers. These liquid crystal cells are observed in a pair of crossed polarizers. The transmitted images are taken in two orientations of the cell, 45° with respect to each other. When the etching time is 0 min, 3.5 min, and 4.0 min, the transmitted images at both 0° and 45° show the same random textures. It means that the alignment of liquid crystal molecules is not aligned well. On the other hand, for three liquid crystal cells with etching times, 2.0 min, 2.5 min and 3.0 min, the liquid crystal cells show the dark state at both 0° and 45°. It indicates that only the AAO thin films manufacturing by these three conditions can perform as the vertical alignment layers. When the etching time is 1.5 min, 5.0 min, and 6.0 min, there is an unexpected result. The transmitted images show a dark state at 0° and a white state at 45°. It shows the homogenous alignment characterization and is different from the other liquid crystal cells with the AAO alignment layers. For the further investigation of the alignment characterization, the conoscopic images were taken.

Figure 6(c) shows the conoscopic images of the same liquid crystal cells with the etched AAO alignment layers. In principle, the cross or parabolic textures show that

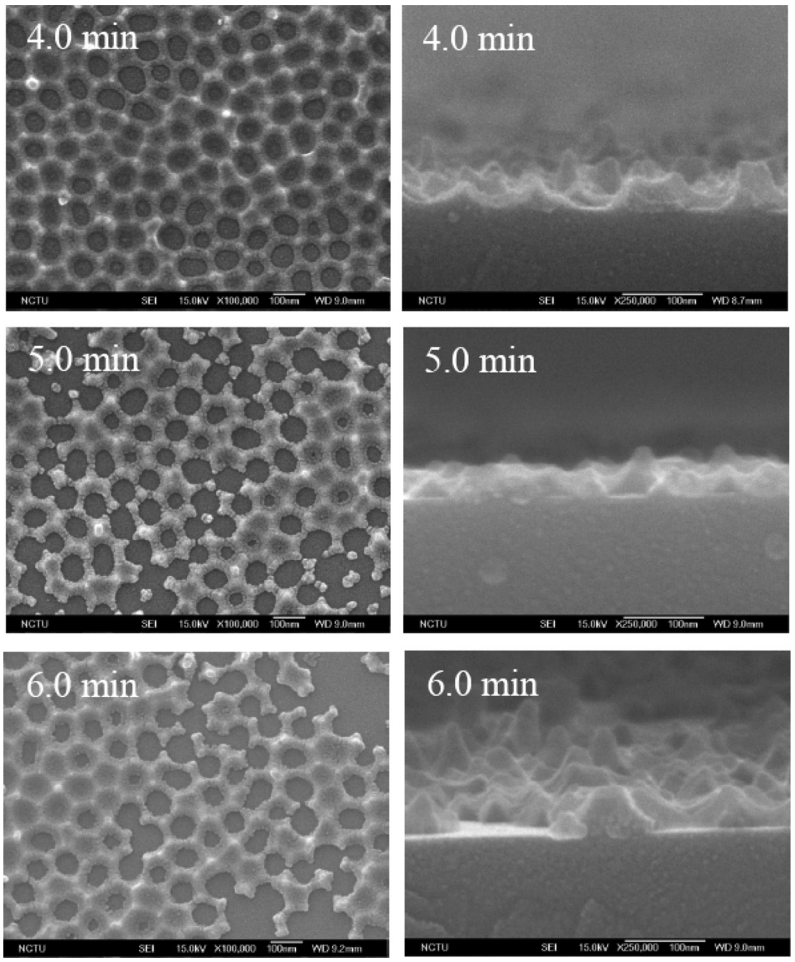

Figure 2 (Part 3). Continued, with etching time, 4.0 min, 5.0 min, and 6.0 min.

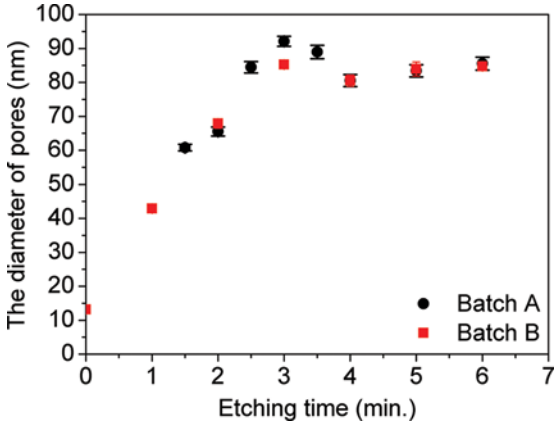

Figure 3. The relationship between the diameter of pores and the etching time. (Figure appears in color online.)

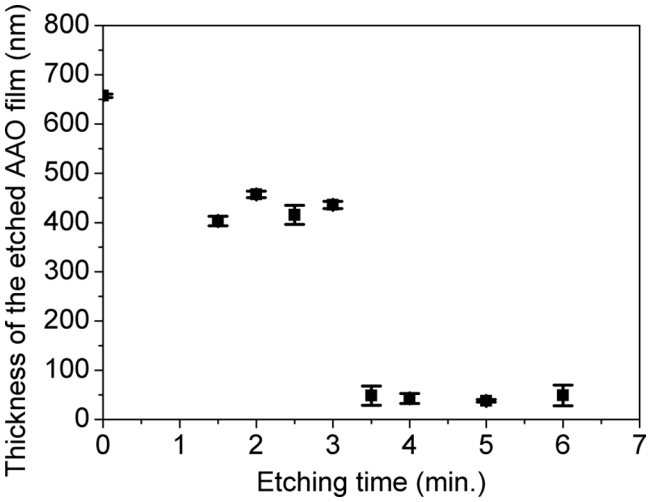

Figure 4. Thickness of the etched AAO thin films with different etching time.

the liquid crystal cell was vertically or homogenously aligned, respectively. In Figure 6(c), the cross textures are shown for the liquid crystal cell with etching times, 2.5 min, 3.0 min, and 3.5 min. It is consistent with the transmitted images and indicates that these three liquid crystal cell are good vertical alignment cell. For 1.5 min, 5.0 min, and 6.0 min, they are neither the cross texture nor the parabolic texture and the alignment characterizations are not clearly sure, yet. Further research about the alignment mechanism has been progressed.

3.4. *Polar Anchoring Strength Analysis*

According to the previous section, the etched AAO thin film with the etching time from 2.0 min to 3.0 min can vertically align nematic liquid crystal. In order to characterize the alignment ability of the etched AAO thin film, the polar anchoring strength has been measured. The polar anchoring strength is measured by using

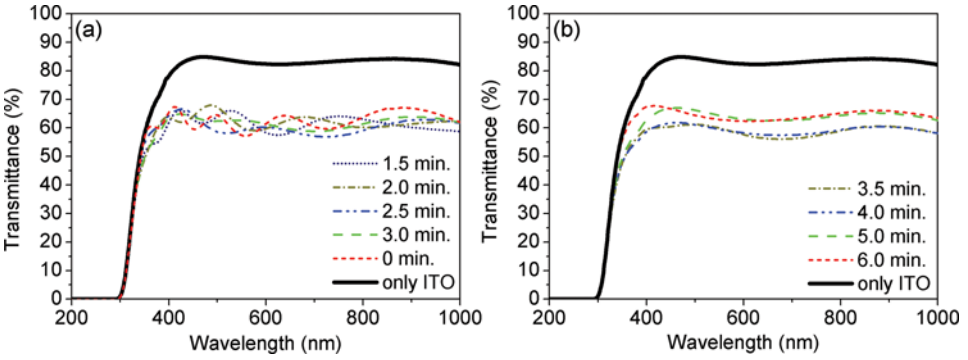

Figure 5. Transmittance of the ITO substrates with the etched AAO films with different etching time. (Figure appears in color online.)

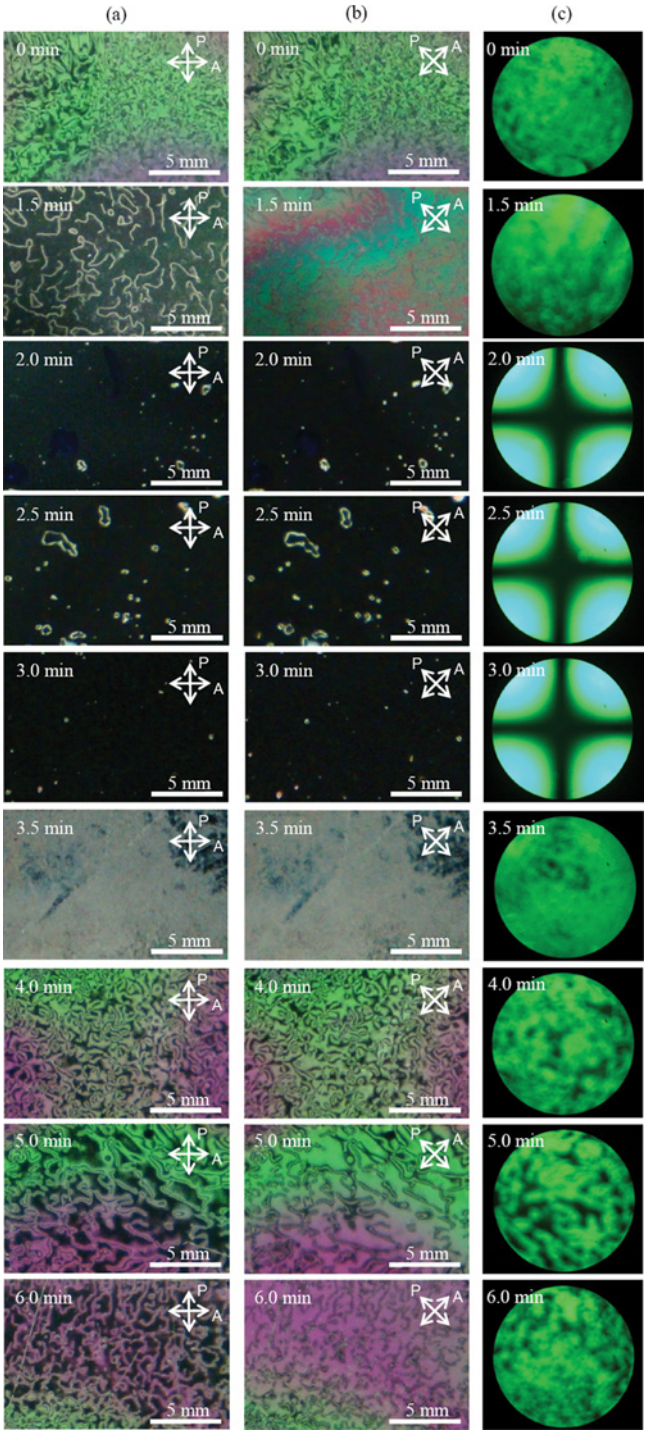

Figure 6. (a) The polarizing transmitted images at 0°, (b) at 45° and (c) the conoscopic images of the liquid crystal cells with the etched AAO thin film as the alignment layer. (Figure appears in color online.)

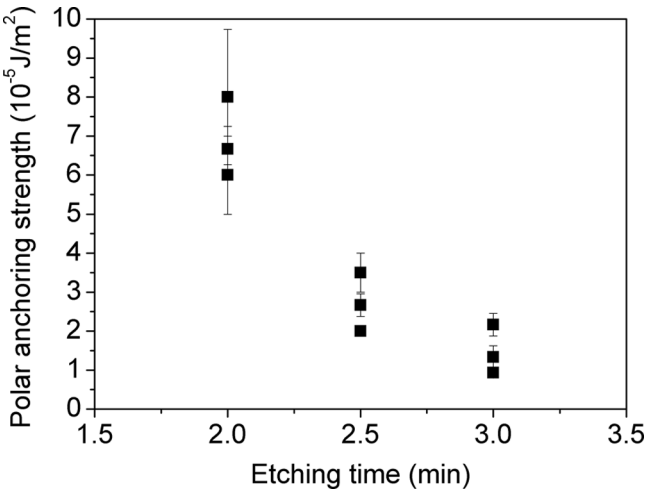

Figure 7. The relationship between the polar anchoring strength and the etching time.

the magnetic field method [27]. The beam size of the detected light in the polar anchoring strength measurement is around 1 mm, and the selected area is uniform and without any defects. Figure 7 shows the relationship between the polar anchoring strengths of the liquid crystal cell cells and the etching times of these cells are 2.0 min, 2.5 min and 3.0 min. In Figure 7, the data dots are the average anchoring strength, and the error is the standard deviation. The different data dots with the same etching time are the polar anchoring strength in different liquid crystal cell with the AAO alignment layer with the same etching time. It clearly shows the etched AAO thin films with shorter etching time have stronger polar anchoring strength. The aspect ratio can be defined as the thickness of the etched AAO thin film divided by the diameter of pores. According to Figures 3 and 4, the relationship between the polar anchoring strength and the aspect ratio can be redrawn as shown in

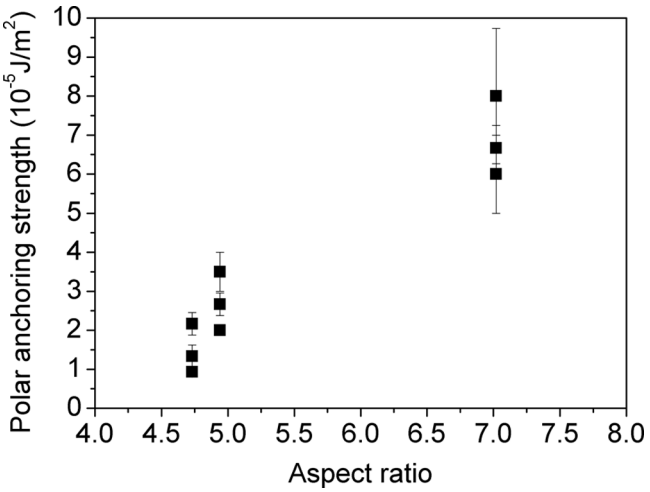

Figure 8. The relationship between the polar anchoring strength and the aspect ratio.

Figure 8. It clearly shows that the etched AAO thin film with higher aspect ratio has higher polar anchoring strength.

3.3.5. *Possible Alignment Mechanism*

The alignment of liquid crystal molecules depend on the surface morphology and the surface tension energy. Depending on the surface tension energy of the AAO material, the liquid crystal molecules tend to align parallel to the AAO surface. The aspect ratio R is defined as thickness/diameter, $l/2r$. Considering a perfect cylinder, the total area of the wall is $2\pi rl$, where r and l are the radius and depth of the cylinder, respectively. The total area can be rewritten as $4\pi r^2 R$. Assuming the pore sizes are constant, the porous AAO thin films with higher aspect ratio have larger surface area at out-of-plane direction. The liquid crystal molecules are affected by the AAO surface at not only in-plane but also out-of-plane direction. Therefore, the alignments of liquid crystal molecules depend on the ratio of the in-plane area to out-of-plane area of the porous AAO surface. The surface property of the AAO material is dominated the alignment property, and the porous structures modify the alignment ability. For porous AAO thin films which contain high aspect ratio pores array, the area at out-of-plane direction is much larger than that at in-plane direction. The liquid crystal molecules are aligned homeotropically by the out-of-plane surfaces. Resulting in the AAO thin films are as the vertical alignment layer. However, when the etching time is 1.5 min, the smaller pores can not fill in the liquid crystal. The liquid crystal cell exhibits as a homogenous alignment cell. For 5.0 min, and 6.0 min, most of the pore array has been etched, and the liquid crystal molecules align parallel to the substrate. It is the most possible alignment mechanism of liquid crystal on the porous AAO thin film.

4. Conclusions

The morphology and the alignment properties of the etched AAO films with different etching time have been investigated. Because the etching process is perpendicular to the AAO surface, both the thickness and the pores diameter of the etched AAO thin film can be modified, and the aspect ratio is controllable. When the etched walls of the AAO pores are too thin, the wall will collapse, and the hexagonal pores array will be removed. The hexagonal curve surface can not perform as the alignment layer. Both homeotropic and homogenous alignment properties are observed on the etched AAO thin films. The AAO thin film with higher aspect ratio has higher polar anchoring strength. The further research about the mechanism of the alignment on the etched AAO thin film is under processed.

Acknowledgment

This work was supported by National Science Council, Republic of China, under grand number 96-2221-E-009-131-MY3.

References

[1] Nakamura, M. (1981). *J. Appl. Phys.*, *52*, 4561.
[2] Chaudhari, P., Lacey, J., Doyle, J., Galligan, E., Alan Lien, S. C., Callegari, A., Hougham, G., Lang, N. D., Andry, P. S., John, R., Yang, K. H., Lu, M., Cai, C.,

Speidell, J., Purushothaman, S., Ritsko, J., Samant, M., Stöhr, J., Nakagawa, Y., Katoh, Y., Saitoh, Y., Sakai, K., Satoh, H., Odahara, S., Nakano, H., Nakagaki, J., & Shiota, Y. (2001). *Nature*, *411*, 56.
[3] Wu, H. Y., Tang, T. T., Wang, C. C., Pan, R. P., Chang, S. J., & Hwang, J. C. (2007). *Mol. Cryst. Liq. Cryst.*, *475*, 45.
[4] Pan, R. P., Chiu, H. Y., Lin, Y. F., & Huang, J. Y. (2003). *Chinese J. Phys.*, *41*, 177.
[5] Yaroshchuk, O., Cada, L. G., Sonpatki, M., & Chien, L.-C. (2001). *Appl. Phys. Lett.*, *79*, 30.
[6] Berreman, D. W. (1972). *Phys. Rev. Lett.*, *28*, 1683.
[7] Faetti, S. (1987). *Phys. Rev. A*, *36*, 408.
[8] Lin, Y. F., Lu, S. Y., & Pan, R. P. (2005). *Jpn. J. Appl. Phys.*, *44*, 8552.
[9] Lin, Y. F., Tsou, M. C., & Pan, R. P. (2005). *Chinese J. Phys.*, *43*, 1066.
[10] Faetti, S., Gatti, M., Palleschi, V., & Sluckin, T. J. (1985). *Phys. Rev. Lett.*, *55*, 1681.
[11] Yokoyama, H., Kobayashi, S., & Kamei, H. (1987). *J. Appl. Phys.*, *61*, 4501.
[12] Janning, J. L. (1972). *Appl. Phys. Lett.*, *21*, 173.
[13] Keller, F., Hunter, M. S., & Robinson, D. L. (1953). *J. Electrochem. Soc.*, *100*, 411.
[14] Jessensky, O., Müller, F., & Gösele, U. (1998). *Appl. Phys. Lett.*, *72*, 1173.
[15] Li, A. P., Müller, F., Bimer, A., Nielsch, K., & Gösele, U. (1998). *J. Appl. Phys.*, *84*, 6023.
[16] Li, A. P., Müller, F., Bimer, A., Nielsch, K., & Gösele, U. (1999). *J. Vac. Sci. Technol. A*, *17*, 1428.
[17] Masuda, H., & Fukuda, K. (1995). *Science*, *268*, 1466.
[18] Masuda, H., Hasegawa, F., & Ono, S. (1997). *J. Electrochem. Soc.*, *144*, L127.
[19] Kyotani, T., Tsai, L. F., & Tomita, A. (1996). *Chem. Mater.*, *8*, 2109.
[20] Routkevitch, D., Bigioni, T., Moskovits, M., & Xu, J. M. (1996). *J. Phys. Chem.*, *100*, 14037.
[21] Al-Mawlawi, D., Liu, C. Z., & Moskovits, M. (1994). *J. Mater. Res.*, *9*, 1014.
[22] Maeda, T., & Hiroshima, K. (2004). *Jpn. J. Appl. Phys.*, *43*, L1004.
[23] Maeda, T., & Hiroshima, K. (2005). *Jpn. J. Appl. Phys.*, *44*, L845.
[24] Tang, T. T., Kuo, C. Y., Pan, R. P., Shieh, J. M., & Pan, C. L. (2009). *J. Display Technol.*, *5*, 350.
[25] Hong, C., Tang, T. T., Hung, C. Y., Pan, R. P., & Fang, W. (2010). *Nanotechnology*, *21*, 285201.
[26] Van Horn, B. L., & Winter, H. H. (2001). *Applied Optics*, *40*, 2089.
[27] Yang, K. H., & Rosenblatt, C. (1983). *Appl. Phys. Lett. 43*, 62.